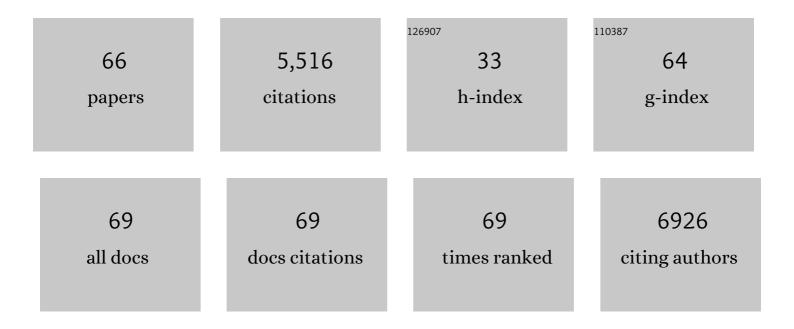
List of Publications by Year in descending order

Source: https://exaly.com/author-pdf/6478395/publications.pdf Version: 2024-02-01



SONG HONG

#	Article	IF	CITATIONS
1	Nitrogen Fixation by Ru Single-Atom Electrocatalytic Reduction. CheM, 2019, 5, 204-214.	11.7	739
2	Highly Conductive Transition Metal Carbide/Carbonitride(MXene)@polystyrene Nanocomposites Fabricated by Electrostatic Assembly for Highly Efficient Electromagnetic Interference Shielding. Advanced Functional Materials, 2017, 27, 1702807.	14.9	620
3	Role of Sulfur Vacancies and Undercoordinated Mo Regions in MoS ₂ Nanosheets toward the Evolution of Hydrogen. ACS Nano, 2019, 13, 6824-6834.	14.6	402
4	Structure of the catalytically active copper–ceria interfacial perimeter. Nature Catalysis, 2019, 2, 334-341.	34.4	368
5	Platinum–copper single atom alloy catalysts with high performance towards glycerol hydrogenolysis. Nature Communications, 2019, 10, 5812.	12.8	277
6	Activated TiO2 with tuned vacancy for efficient electrochemical nitrogen reduction. Applied Catalysis B: Environmental, 2019, 257, 117896.	20.2	220
7	Activation of Ni Particles into Single Ni–N Atoms for Efficient Electrochemical Reduction of CO ₂ . Advanced Energy Materials, 2020, 10, 1903068.	19.5	210
8	Carbon-supported Ni nanoparticles for efficient CO ₂ electroreduction. Chemical Science, 2018, 9, 8775-8780.	7.4	179
9	Preparation of Fe–N–C catalysts with FeN _x (<i>x</i> = 1, 3, 4) active sites and comparison of their activities for the oxygen reduction reaction and performances in proton exchange membrane fuel cells. Journal of Materials Chemistry A, 2019, 7, 26147-26153.	10.3	172
10	Au ^{δâ^'} –O _v –Ti ³⁺ Interfacial Site: Catalytic Active Center toward Low-Temperature Water Gas Shift Reaction. ACS Catalysis, 2019, 9, 2707-2717.	11.2	153
11	Oxygen vacancy enables electrochemical N2 fixation over WO3 with tailored structure. Nano Energy, 2019, 62, 869-875.	16.0	150
12	Photocatalytic Fixation of Nitrogen to Ammonia by Single Ru Atom Decorated TiO ₂ Nanosheets. ACS Sustainable Chemistry and Engineering, 2019, 7, 6813-6820.	6.7	142
13	Highly stable two-dimensional bismuth metal-organic frameworks for efficient electrochemical reduction of CO2. Applied Catalysis B: Environmental, 2020, 277, 119241.	20.2	109
14	Stabilization of Cu ⁺ by tuning a CuO–CeO ₂ interface for selective electrochemical CO ₂ reduction to ethylene. Green Chemistry, 2020, 22, 6540-6546.	9.0	98
15	High-yield production of few-layer boron nanosheets for efficient electrocatalytic N ₂ reduction. Chemical Communications, 2019, 55, 4246-4249.	4.1	96
16	Aqueous CO ₂ Reduction with High Efficiency Using αâ€Co(OH) ₂ â€5upported Atomic Ir Electrocatalysts. Angewandte Chemie - International Edition, 2019, 58, 4669-4673.	13.8	90
17	Interfacial Fe5C2-Cu catalysts toward low-pressure syngas conversion to long-chain alcohols. Nature Communications, 2020, 11, 61.	12.8	78
18	New solvent-stabilized few-layer black phosphorus for antibacterial applications. Nanoscale, 2018, 10, 12543-12553.	5.6	74

#	Article	IF	CITATIONS
19	Highly-efficient RuNi single-atom alloy catalysts toward chemoselective hydrogenation of nitroarenes. Nature Communications, 2022, 13, .	12.8	68
20	ZIF-67-Derived Cobalt/Nitrogen-Doped Carbon Composites for Efficient Electrocatalytic N ₂ Reduction. ACS Applied Energy Materials, 2019, 2, 6071-6077.	5.1	67
21	Atomically Dispersed Au on In ₂ O ₃ Nanosheets for Highly Sensitive and Selective Detection of Formaldehyde. ACS Sensors, 2020, 5, 2611-2619.	7.8	67
22	Single Sb sites for efficient electrochemical CO ₂ reduction. Chemical Communications, 2019, 55, 12024-12027.	4.1	65
23	Reduced graphene oxides with engineered defects enable efficient electrochemical reduction of dinitrogen to ammonia in wide pH range. Nano Energy, 2020, 68, 104323.	16.0	64
24	NiS ₂ nanodotted carnation-like CoS ₂ for enhanced electrocatalytic water splitting. Chemical Communications, 2019, 55, 3781-3784.	4.1	56
25	Ultrasound-Assisted Nitrogen and Boron Codoping of Graphene Oxide for Efficient Oxygen Reduction Reaction. ACS Sustainable Chemistry and Engineering, 2019, 7, 3434-3442.	6.7	49
26	Graphene quantum dots as the electrolyte for solid state supercapacitors. Scientific Reports, 2016, 6, 19292.	3.3	46
27	Efficient visible-light driven N ₂ fixation over two-dimensional Sb/TiO ₂ composites. Chemical Communications, 2019, 55, 7171-7174.	4.1	46
28	Insight into the Role of Unsaturated Coordination O _{2c} -Ti _{5c} -O _{2c} Sites on Selective Glycerol Oxidation over AuPt/TiO ₂ Catalysts. ACS Catalysis, 2019, 9, 188-199.	11.2	45
29	Efficient Electrochemical Reduction of CO ₂ by Ni–N Catalysts with Tunable Performance. ACS Sustainable Chemistry and Engineering, 2019, 7, 15030-15035.	6.7	40
30	Singleâ€Atom Catalyst Aggregates: Sizeâ€Matching is Critical to Electrocatalytic Performance in Sulfur Cathodes. Advanced Science, 2022, 9, e2103773.	11.2	40
31	Enhanced electrochemical CO2 reduction to ethylene over CuO by synergistically tuning oxygen vacancies and metal doping. Cell Reports Physical Science, 2021, 2, 100356.	5.6	39
32	Integration of ultrafine CuO nanoparticles with two-dimensional MOFs for enhanced electrochemical CO2 reduction to ethylene. Chinese Journal of Catalysis, 2022, 43, 1049-1057.	14.0	39
33	Surface-engineered oxidized two-dimensional Sb for efficient visible light-driven N2 fixation. Nano Energy, 2020, 78, 105368.	16.0	37
34	Single atom and defect engineering of CuO for efficient electrochemical reduction of CO ₂ to C ₂ H ₄ . SmartMat, 2022, 3, 194-205.	10.7	34
35	Simultaneous Improvement in Both Electrical Conductivity and Toughness of Polyamide 6 Nanocomposites Filled with Elastomer and Carbon Black Particles. Industrial & Engineering Chemistry Research, 2014, 53, 2270-2276.	3.7	33
36	Ir Single Atom Catalyst Loaded on Amorphous Carbon Materials with High HER Activity. Advanced Science, 2022, 9, e2105392.	11.2	33

#	Article	IF	CITATIONS
37	Synergistic catalysis of CuO/In ₂ O ₃ composites for highly selective electrochemical CO ₂ reduction to CO. Chemical Communications, 2019, 55, 12380-12383.	4.1	32
38	Single yttrium sites on carbon-coated TiO ₂ for efficient electrocatalytic N ₂ reduction. Chemical Communications, 2020, 56, 10910-10913.	4.1	31
39	Selective Catalytic Oxidation of Methane to Methanol in Aqueous Medium over Copper Cations Promoted by Atomically Dispersed Rhodium on TiO ₂ . Angewandte Chemie - International Edition, 2022, 61, e202201540.	13.8	29
40	Liquid Exfoliation of Two-Dimensional Pbl ₂ Nanosheets for Ultrafast Photonics. ACS Photonics, 2019, 6, 1051-1057.	6.6	28
41	Tuning the Pd-catalyzed electroreduction of CO ₂ to CO with reduced overpotential. Catalysis Science and Technology, 2018, 8, 3894-3900.	4.1	24
42	Can closed shell graphitic materials be exfoliated? Defect induced porphyra-like graphene from the cooperation of activation and oxidation. Journal of Materials Chemistry A, 2013, 1, 14103.	10.3	23
43	Review of the Principles, Devices, Parameters, and Applications for Centrifugal Electrospinning. Macromolecular Materials and Engineering, 2022, 307, .	3.6	22
44	Interface engineered Sb2O3/W18O49 heterostructure for enhanced visible-light-driven photocatalytic N2 reduction. Chemical Engineering Journal, 2022, 438, 135485.	12.7	21
45	Aqueous CO ₂ Reduction with High Efficiency Using α o(OH) ₂ â€&upported Atomic Ir Electrocatalysts. Angewandte Chemie, 2019, 131, 4717-4721.	2.0	20
46	Robust, Superelastic Hard Carbon with In Situ Ultrafine Crystals. Advanced Functional Materials, 2020, 30, 1907486.	14.9	20
47	Atomically dispersed ruthenium sites on whisker-like secondary microstructure of porous carbon host toward highly efficient hydrogen evolution. Journal of Materials Chemistry A, 2020, 8, 3203-3210.	10.3	20
48	Understanding the Morphology of High-Performance Solar Cells Based on a Low-Cost Polymer Donor. ACS Applied Materials & Interfaces, 2020, 12, 9537-9544.	8.0	17
49	Atomically Dispersed Nickel Sites for Selective Electroreduction of CO ₂ . ACS Applied Energy Materials, 2019, 2, 8836-8842.	5.1	16
50	Biomimetic caged platinum catalyst for hydrosilylation reaction with high site selectivity. Nature Communications, 2021, 12, 64.	12.8	16
51	Engineering vacancy and hydrophobicity of two-dimensional TaTe2 for efficient and stable electrocatalytic N2 reduction. Innovation(China), 2022, 3, 100190.	9.1	16
52	Fabrication of a compressible PU@RGO@MnO ₂ hybrid sponge for efficient removal of methylene blue with an excellent recyclability. RSC Advances, 2016, 6, 88897-88903.	3.6	15
53	Interlayer confinement synthesis of Ir nanodots/dual carbon as an electrocatalyst for overall water splitting. Journal of Materials Chemistry A, 2021, 9, 4176-4183.	10.3	14
54	Atomically Dispersed Pt on Three-Dimensional Ordered Macroporous SnO ₂ for Highly Sensitive and Highly Selective Detection of Triethylamine at a Low Working Temperature. ACS Applied Materials & Interfaces, 2022, 14, 13440-13449.	8.0	14

#	Article	IF	CITATIONS
55	Selective Electroreduction of CO ₂ and CO to C ₂ H ₄ by Synergistically Tuning Nanocavities and the Surface Charge of Copper Oxide. ACS Sustainable Chemistry and Engineering, 2022, 10, 6466-6475.	6.7	13
56	Cadmium-based metalâ^'organic frameworks for high-performance electrochemical CO2 reduction to CO over wide potential range. Chinese Journal of Chemical Engineering, 2022, 43, 143-151.	3.5	12
57	The influence of topology and morphology of fillers on the conductivity and mechanical properties of rubber composites. Journal of Polymer Research, 2018, 25, 1.	2.4	11
58	Controllable preparation of methyltriethoxysilane xerogel nanofibers. Journal of Materials Science, 2019, 54, 10130-10140.	3.7	11
59	Helically twining polymerization for constructing polymeric double helices. Polymer Chemistry, 2017, 8, 5726-5733.	3.9	9
60	Towards Si@SiO ₂ core–shell, yolk–shell, and SiO ₂ hollow structures from Si nanoparticles through a self-templated etching–deposition process. RSC Advances, 2014, 4, 29435-29438.	3.6	8
61	Nickel-Based Single-Atom Catalyst toward Triiodide Reduction Reaction in Hybrid Photovoltaics. ACS Sustainable Chemistry and Engineering, 2021, 9, 4256-4261.	6.7	8
62	Facile synthesis of two-dimensional copper terephthalate for efficient electrocatalytic CO ₂ reduction to ethylene. Journal of Experimental Nanoscience, 2021, 16, 246-254.	2.4	7
63	Coordinately unsaturated O _{2c} –Ti _{5c} –O _{2c} sites promote the reactivity of Pt/TiO ₂ catalysts in the solvent-free oxidation of <i>n</i> -octanol. Catalysis Science and Technology, 2021, 11, 4898-4910.	4.1	6
64	Selective Catalytic Oxidation of Methane to Methanol in Aqueous Medium over Copper Cations Promoted by Atomically Dispersed Rhodium on TiO ₂ . Angewandte Chemie, 0, , .	2.0	3
65	Decrease in viscosity of styreneâ€isopreneâ€styrene filling systems induced by micro elastic phase. Journal of Applied Polymer Science, 2021, 138, 51368.	2.6	2
66	Highly Catalytically Active High-spin Single-atom Iron Catalyst Supported by Catechol-containing Microporous 2D Polymer. Chemistry Letters, 2020, 49, 1240-1244.	1.3	1